Neutral Weak Form Factor Measurements from the PREX-II and CREX Experiments

Allison J. Zec
(she/her)

Univ. of New Hampshire

2022-09-02

PVES and Nuclear Structure

Parity Violating Electron Scattering

- Measure scattering asymmetry from left & right handed polarized electrons:

$$A_{PV} = \frac{\sigma_R - \sigma_L}{\sigma_R + \sigma_L} = \frac{\mathcal{M}_\gamma^* \mathcal{M}_W}{\mathcal{M}_\gamma^2} \quad (1)$$

- First measurement: E122 at SLAC (1978)
- PVES experiments have broad scope
- Also useful in pioneering technology and methods for ensuring beam stability
- Progressively lower asymmetries measured over generations

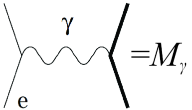

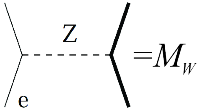

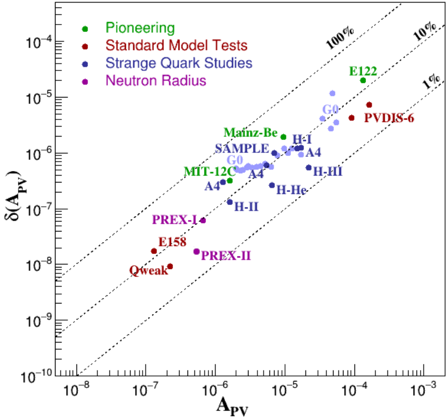

Weak Charge & Neutron Skin

M Thiel *et al* 2019 *J. Phys. G: Nucl. Part. Phys.* **46** 093003

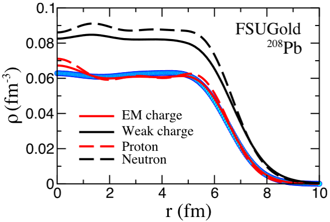

- Theory predicts "neutron skin"
- Excess neutrons pushed radially outwards against surface tension due to pressure of nuclear matter
- Asymmetry correlated with EM & weak form factors:

$$A_{PV} \approx \frac{G_F q^2}{4\pi\alpha\sqrt{2}} \frac{F_W}{F_{ch}} \qquad (2)$$

	Proton	Neutron
EM Charge	1	0
Weak Charge	0.08	1

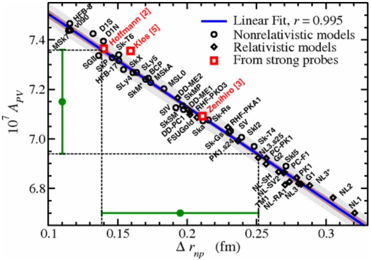

Current theory models predicting neutron radius and asymmetry highly correlated, but not constrained well by neutron radius measurements

X. Roca-Maza *et al* 2011 *Phys. Rev. Lett.* **106** 252501

PREX-II & CREX

	PREX-II	CREX
Target	^{208}Pb	^{48}Ca
Target Thick.	0.5 mm	6 mm
Beam Energy	1 GeV	2.2 GeV
$\langle Q^2 \rangle$	0.00616 GeV^2	0.0297 GeV^2
$\langle \theta \rangle$	5°	5°

Predicted asymmetries on the order of 1 ppm!

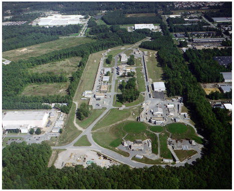

- Two PVES experiments, run at JLab Hall A in 2019-20
- Neutron radius from A_{PV} measurements
- Polarized electron beam on unpolarized high-Z targets
- ^{208}Pb radius: test of uniform nuclear matter
- ^{48}Ca radius: test of different nuclear structure models
- Overall goal: $\approx$3% error on A_{PV}^{208} and A_{PV}^{48}

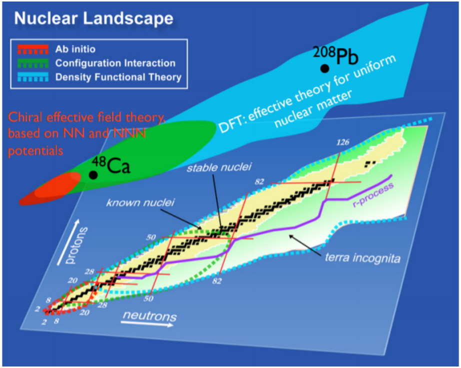

Experimental Apparatus

Polarized Source

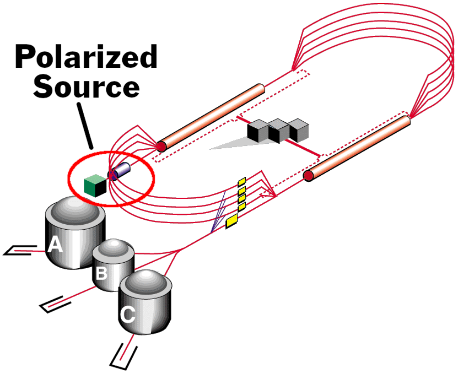

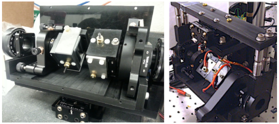

Image Credit: *C. Palatchi (2019)*

Left: RTP pockels cell in its mount. Right: An example of helicity patterns like those used for PREX-II.

- Pockels cell sends circularly polarized laser onto GaAs photocathode
  - Pockels cell controls helicity-flipping
- Insertable Half-Wave Plate independently flips helicity sign
- EM Wien filter also flips helicity (was changed every few weeks)
- Mott polarimeter checks polarization of beam out of injector

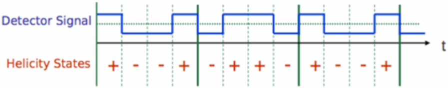

Targets

- One target ladder for both experiments
  - 10 ^{208}Pb targets, 1 ^{48}Ca target
- Multiple ^{208}Pb targets to account for cumulative damage from beam

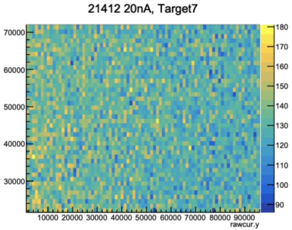

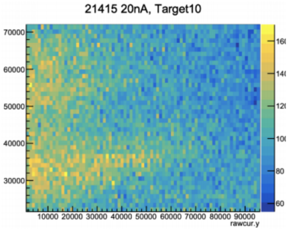

Above Left: *Detector hit distribution from a new ^{208}Pb target*
Above Right: *Detector hit distribution from a damaged ^{208}Pb target*

Right: *The target ladder used during PREX-II and CREX, with target positions labeled*

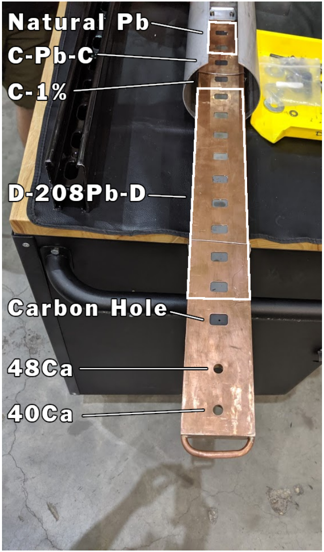

Integrating Detectors:

- Fused silica quartz Čerenkov detectors, two in each spectrometer arm
- Built for beam currents up to 150 μA
- Takes asymmetry data

Counting Detectors:

- VDCs, GEMs and scintillators
- Can only take low current data
- Used for optics, Q^2 measurements, detector alignment, other systematic checks

Right: HRS optics with detectors outlined. Inelastics are steered out of the path of the main detector by the dipole but can still be measured in the counting detectors.

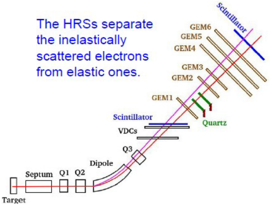

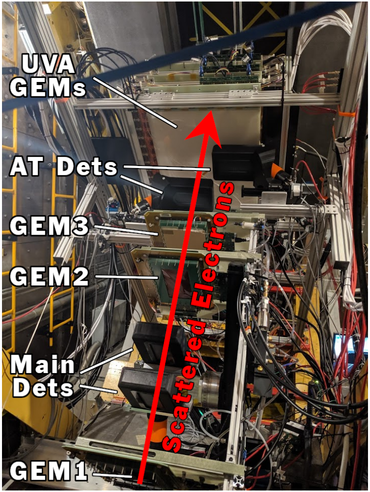

PREX-II/CREX detectors deployed inside the HRS huts

Systematics Controls

Beam Corrections

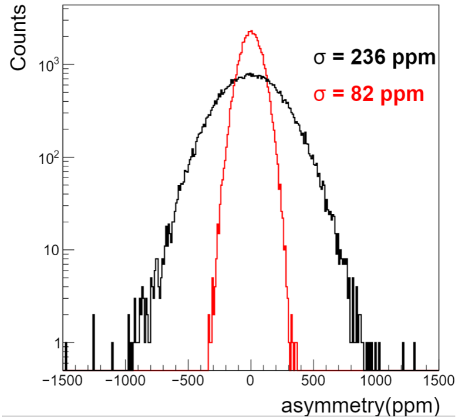

Above: in **black***, the asymmetry distribution without trajectory corrections. In* **red***, the asymmetry distribution with trajectory corrections. (For PREX-II)*

- Uncorrected, the systematic uncertainty from beam backgrounds would be large compared to counting statistics
- Asymmetry correction is:

$$\boxed{A_{PV}} = \boxed{A_{raw} - A_Q} - \sum_i \alpha_i \Delta x_i - \alpha_E A_E \quad (3)$$

- Beam modulation & regression both methods to extract α_i's
- Both modulation and regression data monitored consistently throughout experiments' running

Beam Corrections

Regression

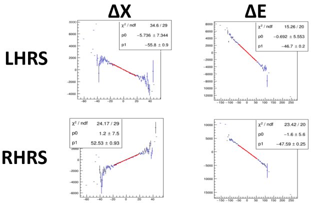

- Position, angle and energy information taken from position monitors
- Trajectories correlated with changes in measured A_{raw}

Modulation

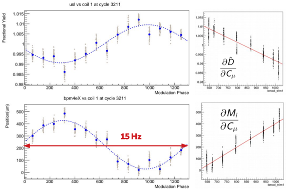

- Magnetic coils alter beam trajectory periodically, in sequence
- Correlation slopes extracted from beam changes

Lagrangian Multipliers

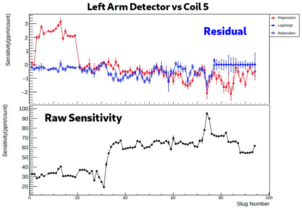

- Create set of Lagrangian multipliers to minimize regression correction
- Constraints come from modulation slopes

Beam Corrections (PREX-II)

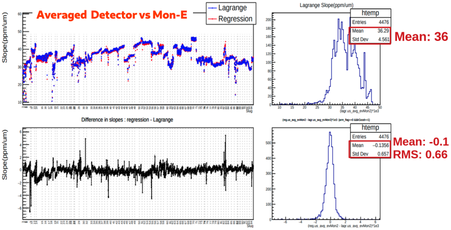

Above: PREX-II regression results. Below: PREX-II regression uncertainty table.

Source	**Mean [ppb]**	**3% Err [ppb]**
E	-70.44	2.11
X1	-22.33	0.67
X2	9.70	0.29
Y1	22.50	0.68
Y2	-2.84	0.06
Others	3.04	0.09
Total	**-60.38**	**2.5**

PREX-II:

- Energy regression is highest source of uncertainty
  - Energy slopes have same sign in L-R HRS detectors and don't cancel out
- Average energy slope: $\sim$36 ppm/μm
- Average difference between Lagrangian and regression slopes: $\sim$0.14 ppm/um
- Determined $\approx$3% uncertainty
  - Determination from difference between regression correcions and Lagrange multiplier corrections

CREX Compton Polarimetry

Image Credit: *D. Jones (2019)*

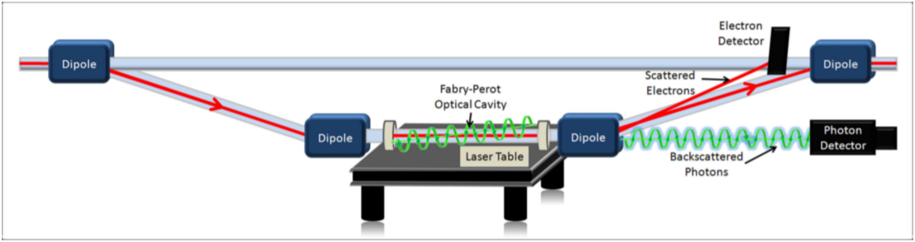

- Polarimeter consists of:
  - Magnetic chicane to steer beam
  - Fabry-Perot cavity on laser table
  - Photon calorimeter
  - High-speed DAQ system
- Laser λ=532 nm

- $\approx$30 MeV Compton edge for PREX-II; $\approx$150 MeV Compton edge for CREX
- Laser polarization measured on table
- Runs concurrently with main experiment

CREX Compton Polarimetry

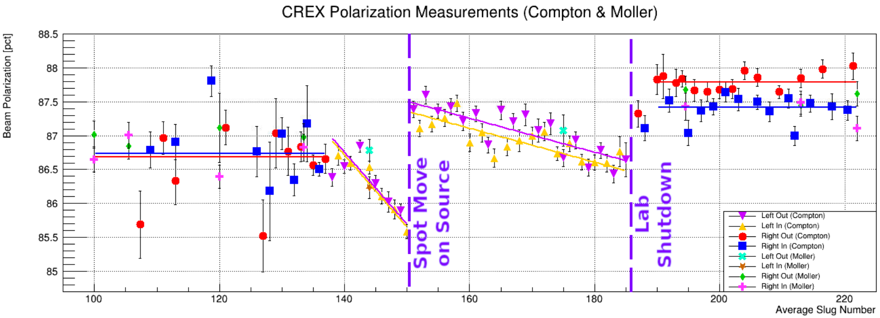

Above: *Møller and Compton polarimetry data for CREX. All uncertainties plotted are statistical only. Møller data courtesy of E. King.*

CREX Compton Polarization

$$\mathcal{P}_e = 87.1\ (\pm 0.44\%\ \text{syst})$$
$$(\pm 0.02\%\ \text{stat})$$

- Time-dependent polarization
- Laser polarization is dominant systematic, followed by photon-cone pointing direction
- Most accurate Compton beam polarimetry measurement

Inelastics Rejection (CREX)

- Hall A HRS's separate inelastics by dipole steering
- Non-tracking "quartz" detectors measure A_{PV}
- Other tracking detectors measure inelastic peak positions

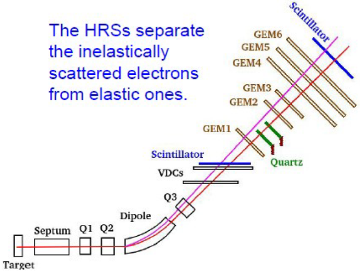

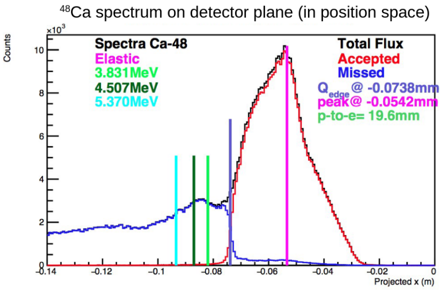

- Frequent detector realignment keeps quartz edge off inelastic peaks
- CREX overall systematic contribution: **0.89%**

Left: *Elastic and inelastic peak locations relative to quartz detector edge*

Image credit: D. Adhikari (2021)

Asymmetry Results

PREX-II Results

PREX-II Asymmetry

$$\mathcal{A}_{PV}^{208} = 550 \pm 16(\text{stats}) \pm 8(\text{syst})$$

parts per billion

Neutron Skin Thickness

$$R_n^{208} - R_p^{208} = 0.283 \pm 0.071 \text{ fm}$$

Uncert. Source	**A_{PV} uncert. contribution**
Polarization	0.95%
Acceptance normalization	0.83%
Beam correction	0.54%
Detector nonlinearity	0.49%
Carbon contamination	0.26%
Charge Correction	0.04%
Inelastic Contamination	0.02%
Total	**1.48%**

PREX-II paper published in PRL!

Phys.Rev.Lett. 126 (2021) 17, 172502

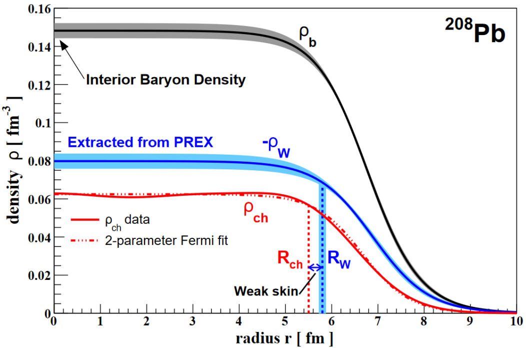

Above: New baryon density curves calculated from PREX-II results.

PREX-II in the News

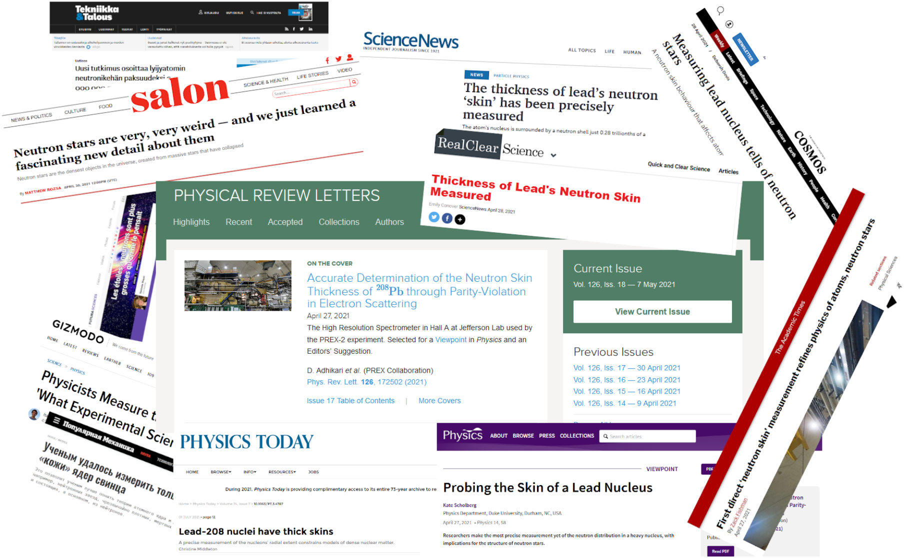

PREX-II in the News

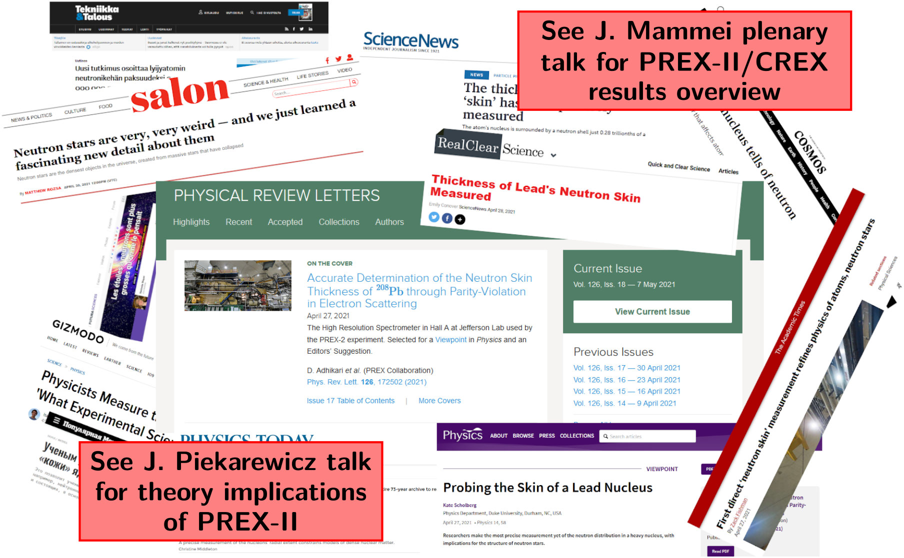

See J. Mammei plenary talk for PREX-II/CREX results overview

See J. Piekarewicz talk for theory implications of PREX-II

CREX Results

CREX Asymmetry

$$\mathcal{A}_{PV}^{48} = 2668 \pm 106(\text{stats}) \pm 39(\text{syst})$$
parts per billion

Neutron Skin Thickness

$$R_n^{48} - R_p^{48} = 0.121 \pm 0.035 \text{ fm}$$

Uncert. Source	**A_{PV} uncert. contribution**
Acceptance normalization	0.90%
Inelastic Contamination	0.82%
Transverse asymmetry	0.49%
Polarization	0.39%
Radiative Corrections	0.37%
Beam Correction	0.27%
Nonlinearity	0.26%
Isotopic purity	0.11%
Total	**1.49%**

Published in PRL! D. Adhikari *et al* Phys. Rev. Lett. **129** 042501

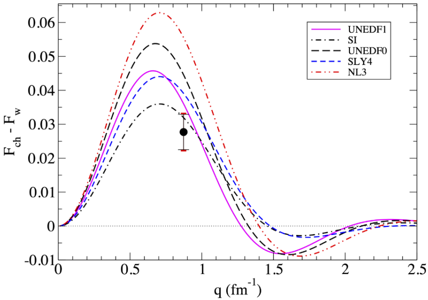

Above: CREX measured $F_{ch} - F_W$ compared to one family of theory models with different weak radii.

Summary

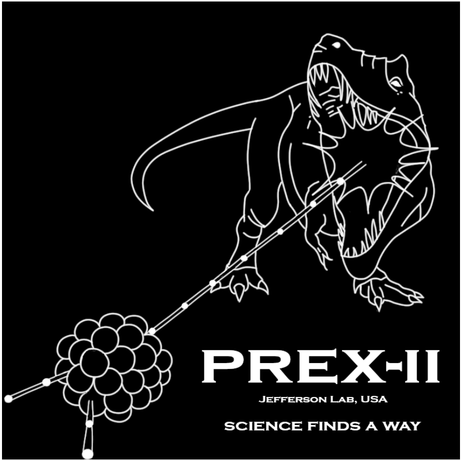

Image Credit: M. Petrusky (2019)

- Two experiments of current PVES generation
  - Reducing and controlling systematic uncertainties from beam
  - Accurate beam polarimetry
  - Specialized “integrating” detectors
- PREX-II ran in summer 2019
- Measured neutron radius of ^{208}Pb
- CREX ran on ^{48}Ca target in spring/summer 2020
- PREX-II and CREX both published in PRL

THANK YOU!

Summary

Accurate Determination of the Neutron Skin Thickness of ^{208}Pb through Parity-Violation in Electron Scattering

(The PREX Collaboration)

D. Adhikari,[1] H. Albataineh,[2] D. Androic,[3] K. Aniol,[4] D.S. Armstrong,[5] T. Averett,[5] C. Ayerbe Gayoso,[5] S. Barcus,[6] V. Bellini,[7] R.S. Beminiwattha,[8] J.F. Benesch,[6] H. Bhatt,[9] D. Bhatta Pathak,[8] D. Bhetuwal,[9] B. Blaikie,[10] Q. Campagna,[5] A. Camsonne,[6] G.D. Cates,[11] Y. Chen,[8] C. Clarke,[12] J.C. Cornejo,[13] S. Covrig Dusa,[6] P. Datta,[14] A. Deshpande,[12,15] D. Dutta,[9] C. Feldman,[12] E. Fuchey,[14] C. Gal,[12,11,15] D. Gaskell,[6] T. Gautam,[16] M. Gericke,[10] C. Ghosh,[17,12] I. Halilovic,[10] J.-O. Hansen,[6] F. Hauenstein,[18] W. Henry,[19] C.J. Horowitz,[20] C. Jantzi,[11] S. Jian,[11] S. Johnston,[17] D.C. Jones,[19] B. Karki,[21] S. Katugampola,[11] C. Keppel,[6] P.M. King,[21] D.E. King,[22] M. Knauss,[23] K.S. Kumar,[17] T. Kutz,[12] N. Lashley-Colthirst,[16] G. Leverick,[10] H. Liu,[17] N. Liyange,[11] S. Malace,[6] J. Mammei,[10] R. Mammei,[24] M. McCaughan,[6] D. McNulty,[1] D. Meekins,[6] C. Metts,[5] R. Michaels,[6] M.M. Mondal,[12,15] J. Napolitano,[19] A. Narayan,[25] D. Nikolaev,[19] M.N.H. Rashad,[18] V. Owen,[5] C. Palatchi,[11,15] J. Pan,[10] B. Pandey,[16] S. Park,[12] K.D. Paschke,[11,*] M. Petrusky,[12] M.L. Pitt,[26] S. Premathilake,[11] A.J.R. Puckett,[14] B. Quinn,[13] R. Radloff,[21] S. Rahman,[10] A. Rathnayake,[11] B.T. Reed,[20] P.E. Reimer,[27] R. Richards,[12] S. Riordan,[27] Y. Roblin,[6] S. Seeds,[14] A. Shahinyan,[28] P. Souder,[22] L. Tang,[6,16] M. Thiel,[29] Y. Tian,[22] G.M. Urciuoli,[30] E.W. Wertz,[5] B. Wojtsekhowski,[6] B. Yale,[5] T. Ye,[12] A. Yoon,[31] A. Zec,[11] W. Zhang,[12] J. Zhang,[12,15,32] and X. Zheng[11]

Precision Determination of the Neutral Weak Form Factor of ^{48}Ca

(The CREX Collaboration)

D. Adhikari,[1] H. Albataineh,[2] D. Androic,[3] K.A. Aniol,[4] D.S. Armstrong,[5] T. Averett,[5] C. Ayerbe Gayoso,[5] S.K. Barcus,[6] V. Bellini,[7] R.S. Beminiwattha,[8] J.F. Benesch,[6] H. Bhatt,[9] D. Bhatta Pathak,[8] D. Bhetuwal,[9] B. Blaikie,[10] J. Boyd,[11] Q. Campagna,[5] A. Camsonne,[6] G.D. Cates,[11] Y. Chen,[8] C. Clarke,[12] J.C. Cornejo,[13] S. Covrig Dusa,[6] M. M. Dalton,[6] P. Datta,[14] A. Deshpande,[12,15,16] D. Dutta,[9] C. Feldman,[12,17] E. Fuchey,[14] C. Gal,[15,9,11,12] D. Gaskell,[6] T. Gautam,[18] M. Gericke,[10] C. Ghosh,[19,12] I. Halilovic,[10] J.-O. Hansen,[6] O. Hassan,[10] F. Hauenstein,[6] W. Henry,[20] C.J. Horowitz,[21] C. Jantzi,[11] S. Jian,[11] S. Johnston,[19] D.C. Jones,[20,6] S. Kakkar,[10] S. Katugampola,[11] C. Keppel,[6] P.M. King,[22] D.E. King,[23,20] K.S. Kumar,[19] T. Kutz,[12] N. Lashley-Colthirst,[18] G. Leverick,[10] H. Liu,[19] N. Liyanage,[11] J. Mammei,[10] R. Mammei,[24] M. McCaughan,[6] D. McNulty,[1] D. Meekins,[6] C. Metts,[5] R. Michaels,[6] M. Mihovilovic,[25,26] M.M. Mondal,[12,15] J. Napolitano,[20] A. Narayan,[27] D. Nikolaev,[20] V. Owen,[5] C. Palatchi,[11,15] J. Pan,[10] B. Pandey,[18] S. Park,[9,12] K.D. Paschke,[11,*] M. Petrusky,[12] M.L. Pitt,[28] S. Premathilake,[11] B. Quinn,[13] R. Radloff,[22] S. Rahman,[10] M.N.H. Rashad,[11] A. Rathnayake,[11] B.T. Reed,[21] P.E. Reimer,[29] R. Richards,[12] S. Riordan,[29] Y.R. Roblin,[6] S. Seeds,[14] A. Shahinyan,[30] P. Souder,[23] M. Thiel,[31] Y. Tian,[23] G.M. Urciuoli,[32] E.W. Wertz,[5] B. Wojtsekhowski,[6] B. Yale,[5] T. Ye,[12] A. Yoon,[33] W. Xiong,[23,34] A. Zec,[11] W. Zhang,[12] J. Zhang,[12,15,34] and X. Zheng[11]

Thank you to our 100+ collaborators!

- Two experiments of current PVES generation
  - Reducing and controlling systematic uncertainties from beam
  - Accurate beam polarimetry
  - Specialized "integrating" detectors
- PREX-II ran in summer 2019
- Measured neutron radius of ^{208}Pb
- CREX ran on ^{48}Ca target in spring/summer 2020
- PREX-II and CREX both published in PRL

THANK YOU!

Summary

Accurate Determination of the Neutron Skin Thickness of ^{208}Pb through Parity

Follow @transphysicists on twitter!

D. Adhikari,[1] H. Albataineh,[2] D. … be Gayoso,[5]
S. Barcus,[6] V. Bellini,[7] R.S. Bemi… Bhetuwal,[9]
B. Blaikie,[10] Q. Campagna,[5] A. Ca… ,[13] S. Covrig
Dusa,[6] P. Datta,[14] A. Deshpande, … D. Gaskell,[6]
T. Gautam,[16] M. Gericke,[10] C. C… Henry,[19]
C.J. Horowitz,[20] C. Jantzi,[11] S… ampola,[11]
C. Keppel,[6] P.M. King,[21] D.E. King,[22] M. Knauss,[23] K.S. Kumar,[17] T. Kutz,[12] N. Lashley-Colthirst,[16]
G. Leverick,[10] H. Liu,[17] N. Liyange,[11] S. Malace,[6] J. Mammei,[10] R. Mammei,[24] M. McCaughan,[6] D. McNulty,[1]
D. Meekins,[6] C. Metts,[5] R. Michaels,[6] M.M. Mondal,[12,15] J. Napolitano,[19] A. Narayan,[25] D. Nikolaev,[19]
M.N.H. Rashad,[18] V. Owen,[5] C. Palatchi,[11,15] J. Pan,[10] B. Pandey,[16] S. Park,[12] K.D. Paschke,[11,*]
M. Petrusky,[12] M.L. Pitt,[26] S. Premathilake,[11] A.J.R. Puckett,[14] B. Quinn,[13] R. Radloff,[21] S. Rahman,[10]
A. Rathnayake,[11] B.T. Reed,[20] P.E. Reimer,[27] R. Richards,[12] S. Riordan,[27] Y. Roblin,[6] S. Seeds,[14]
A. Shahinyan,[28] P. Souder,[22] L. Tang,[6,16] M. Thiel,[29] Y. Tian,[22] G.M. Urciuoli,[30] E.W. Wertz,[5]
B. Wojtsekhowski,[6] B. Yale,[5] T. Ye,[12] A. Yoon,[31] A. Zec,[11] W. Zhang,[12] J. Zhang,[12,15,32] and X. Zheng[11]

Precision Determination of the Neutral Weak Form Factor of ^{48}Ca

(The CREX Collaboration)

D. Adhikari,[1] H. Albataineh,[2] D. Androic,[3] K.A. Aniol,[4] D.S. Armstrong,[5] T. Averett,[5] C. Ayerbe Gayoso,[5]
S.K. Barcus,[6] V. Bellini,[7] R.S. Beminiwattha,[8] J.F. Benesch,[6] H. Bhatt,[9] D. Bhatta Pathak,[8] D. Bhetuwal,[9]
B. Blaikie,[10] J. Boyd,[11] Q. Campagna,[5] A. Camsonne,[6] G.D. Cates,[11] Y. Chen,[8] C. Clarke,[12] J.C. Cornejo,[13]
S. Covrig Dusa,[6] M. M. Dalton,[6] P. Datta,[14] A. Deshpande,[12,15,16] D. Dutta,[9] C. Feldman,[12,17] E. Fuchey,[14]
C. Gal,[15,9,11,12] D. Gaskell,[6] T. Gautam,[18] M. Gericke,[10] C. Ghosh,[19,12] I. Halilovic,[10] J.-O. Hansen,[6] O. Hassan,[10]
F. Hauenstein,[6] W. Henry,[20] C.J. Horowitz,[21] C. Jantzi,[11] S. Jian,[11] S. Johnston,[19] D.C. Jones,[20,6]
S. Kakkar,[10] S. Katugampola,[11] C. Keppel,[6] P.M. King,[22] D.E. King,[23,20] K.S. Kumar,[19] T. Kutz,[12]
N. Lashley-Colthirst,[18] G. Leverick,[10] H. Liu,[19] N. Liyanage,[11] J. Mammei,[10] R. Mammei,[24] M. McCaughan,[6]
D. McNulty,[1] D. Meekins,[6] C. Metts,[5] R. Michaels,[6] M. Mihovilovic,[25,26] M.M. Mondal,[12,15] J. Napolitano,[20]
A. Narayan,[27] D. Nikolaev,[20] V. Owen,[5] C. Palatchi,[11,15] J. Pan,[10] B. Pandey,[18] S. Park,[9,12] K.D. Paschke,[11,*]
M. Petrusky,[12] M.L. Pitt,[28] S. Premathilake,[11] B. Quinn,[13] R. Radloff,[22] S. Rahman,[10] M.N.H. Rashad,[11]
A. Rathnayake,[11] B.T. Reed,[21] P.E. Reimer,[29] R. Richards,[12] S. Riordan,[29] Y.R. Roblin,[6] S. Seeds,[14]
A. Shahinyan,[30] P. Souder,[23] M. Thiel,[31] Y. Tian,[23] G.M. Urciuoli,[32] E.W. Wertz,[5] B. Wojtsekhowski,[6]
B. Yale,[5] T. Ye,[12] A. Yoon,[33] W. Xiong,[23,34] A. Zec,[11] W. Zhang,[12] J. Zhang,[12,15,34] and X. Zheng[11]

Thank you to our 100+ collaborators!

- Two experiments of current PVES generation
    - Reducing and controlling systematic uncertainties from beam
    - Accurate beam polarimetry
    - Specialized "integrating" detectors
- PREX-II ran in summer 2019
- Measured neutron radius of ^{208}Pb
- CREX ran on ^{48}Ca target in spring/summer 2020
- PREX-II and CREX both published in PRL

THANK YOU!

Backup Slides

^{208}Pb

- ^{208}Pb: neutron rich double-magic nucleus
- Can be modeled as uniform nuclear matter
  - Becomes an terrestrial laboratory to test neutron star structure
- Δr_{np} highly correlated to symmetry energy

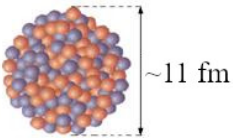

Image Credit: *F. J. Fattoyev (2018)*

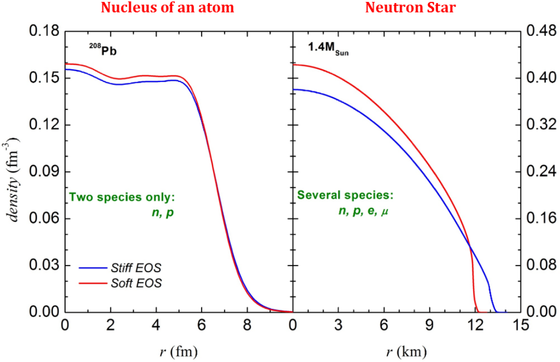

- Neutron star radius 18 orders of magnitude greater than ^{208}Pb radius
- . . . but they have the same EOS!

Pockels Cell Details

- Changed cell crystal to RTP for lower T_{settle} and higher flip rate
- Handled intensity asymmetries with aggressive feedback program
  - Also with careful alignment of crystal
- Separate feedback system for handling position differences off the injector
- Avoid spot-size asymmetries with crystal alignment

(Rubidium Titanyle Phosphate)

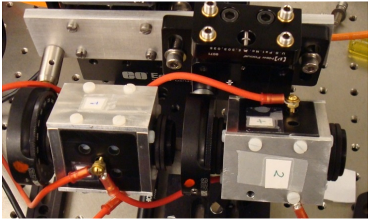

PREX-II Møller Polarimetry

PREX-II Polarization

$\mathcal{P}_e = 89.7$

$(\pm 0.89\%$ syst$)$

$(\pm 0.13\%$ stat$)$

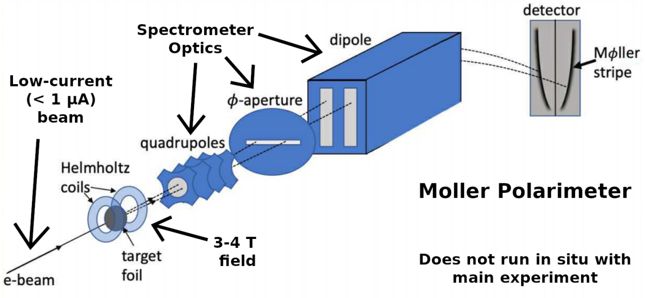

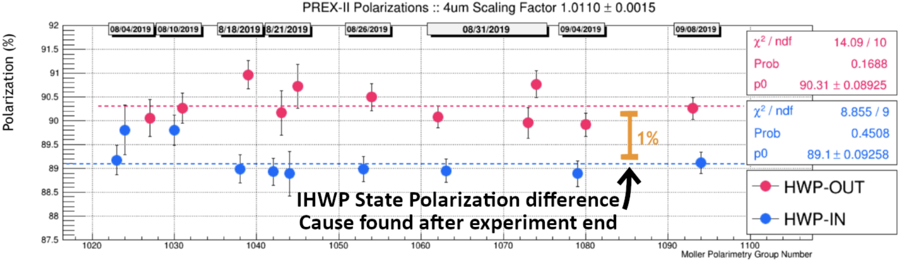

Images courtesy of E. King (2019)

PREX Polarimetry Results

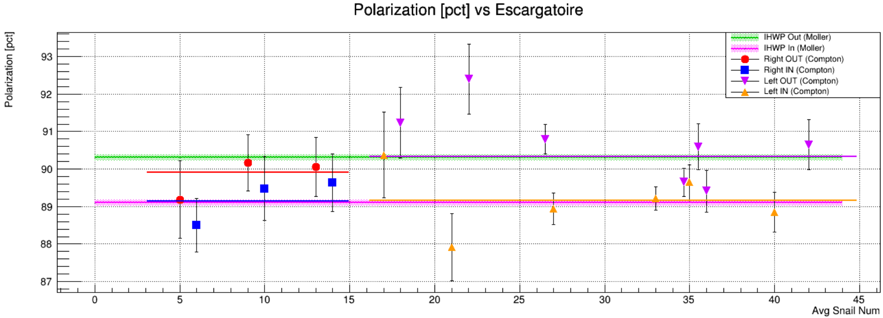

PREX-II Compton results with Møller polarimeter results overlaid in colored bars (stat error only)

- Systematic corrections applied
- Good consistency with Møller (within 0.8% systematic window)
- Compton raw statistics: 0.2%-0.5%
- χ^2 uneven across run periods
- Non-statistical behavior between run periods
- Percent-level polarization changes not yet explained

Inelastics Rejection (PREX-II)

- Additional excited states had contribution to PREX-II
- Inelastic peak detector location further from quartz edge
- Uncertainty introduced from PREX-II elastics is negligible

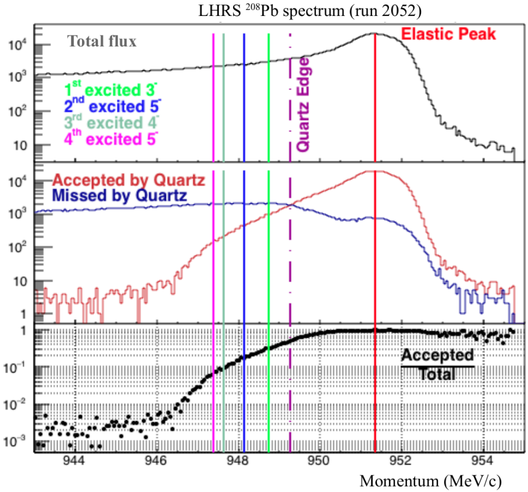

Above: *Inelastic peak spectrum for ^{208}Pb. Image courtesy of D. Adhikari (2021)*

Q^2 & Pointing Angle

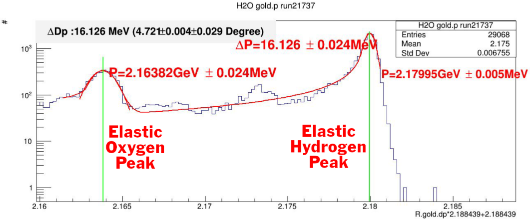

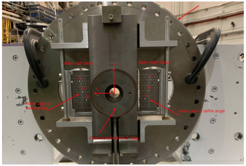

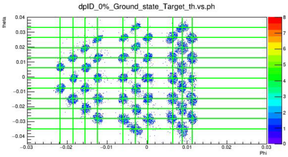

- Angle reconstruction with sieve runs and runs with water cell target
- Q^2 measurement from scattered electron track reconstruction

$$A_{PV} \approx \frac{G_F Q^2}{4\pi\alpha\sqrt{2}} \frac{Q_W}{Z} \frac{F_W(Q^2)}{F_{ch}(Q^2)} \tag{4}$$

$$Q^2 = 4E'^2 f_r sin^2(\frac{\theta}{2}) \tag{5}$$

LHRS Angle	RHRS Angle	Q^2
$(4.765 \pm 0.016)^\circ$	$(4.747 \pm 0.018)^\circ$	$(0.00616 \pm 0.00004)GeV^2$

Carbon Contamination (PREX-II)

Variable	Amount
$\frac{A_{corr}}{P_e}$ [ppb]	549.34
A_c [ppb]	539.36
δA_c [ppb]	21.574
$\frac{\delta A_c}{A_c}$ [%]	4.00
f_c	6.29E-02
δf_c	4.63E-03
Rel. Error from f_c [%]	0.01
Rel. Error from A_c [%]	**0.26**

- Correction for a false asymmetry source can be applied by

$$A_{PV} = \frac{\frac{A_{corr}}{P_e} - \sum_i A_i f_i}{1 - \sum_i f_i} \qquad (6)$$

- Where A_i every source of false asymmetry, f_i is the background fraction, and P_e is the incoming beam polarization
- Theoretical C-asymmetry calculation provided by optical simulation and rate informs correction
- In limit that $\frac{A_{corr}}{P_e} \simeq A_c$ then correction factor approaches 1

Null Asymmetry

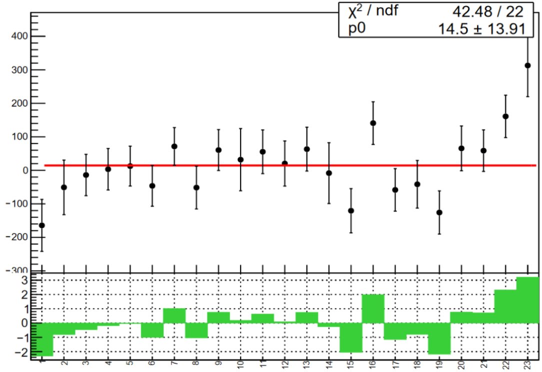

Above: Asymmetry plotted by combined IHWP IN/OUT periods.

- Search for systematic effects by measuring

$$A_{null} = \frac{A_{PV}^{IN} - A_{PV}^{OUT}}{2} \quad (7)$$

- Which should be identically zero without uncorrected systematics.
- Asymmetries should cancel out as IHWP change is just a change of sign
- Average A_{null} zero over PREX-II run

PREX-II and Neutron Stars

- PREX-II has significant implications for the deformability of neutron stars
- NICER experiment bounds the radii of neutron stars
- PREX-II result has good agreement with NICER bounds

Right: the overlap between the PREX-II and NICER error bars is marked in blue in the "Allowed" region

Image Credit: *B. Reed et. al.*

Phys.Rev.Lett. 126 (2021) 17, 172503

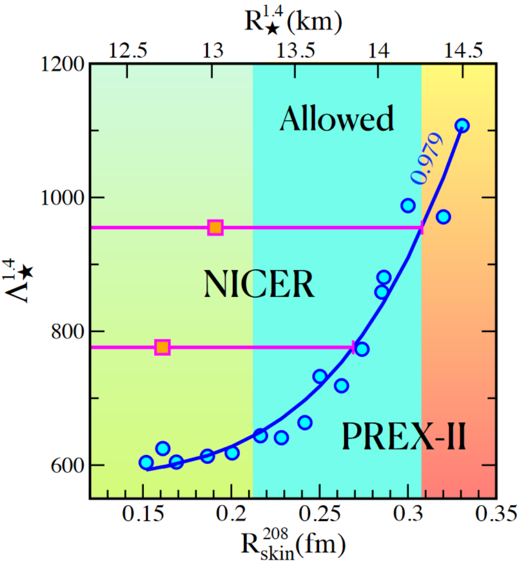

What’s Next for PVES?

MOLLER

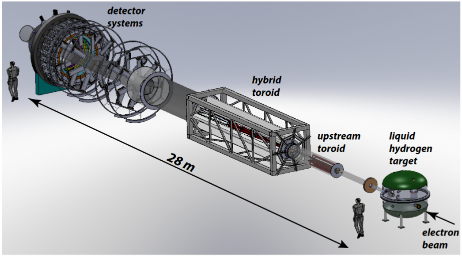

Above: Target, magnet, and detector concept for MOLLER experiment. Image courtesy of MOLLER collaboration.

- High precision measurement of weak mixing angle at low Q^2
- Expected $\mathcal{A}_{PV} \approx 35.6$ ppb

SoLID

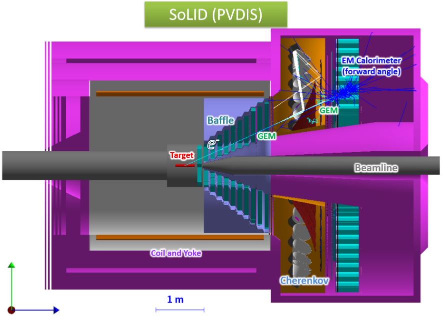

Above: CAD model of SoLID detector in its PVDIS configuration.

- High-luminosity, large acceptance detector
- SIDIS, PVDIS, and J/ψ programs

What's Next for PVES?

MOLLER

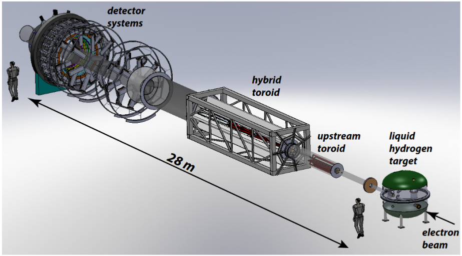

Above: Target, magnet, and detector concept for MOLLER experiment. Image courtesy of MOLLER collaboration.

- High precision measurement of weak mixing angle at low Q^2
- Expected $\mathcal{A}_{PV} \approx$35.6 ppb

SoLID

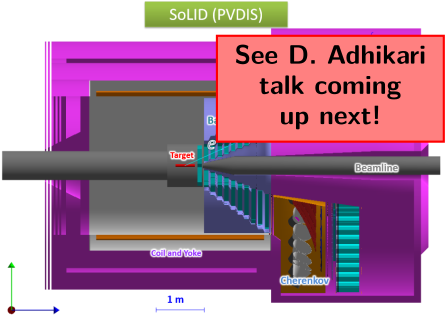

Above: CAD model of SoLID detector in its PVDIS configuration.

- High-luminosity, large acceptance detector
- SIDIS, PVDIS, and J/ψ programs

What's Next for PVES?

- Mainzer Microtron (MAMI) facility in Germany
- Two experiments:
  - **P2:** Ultra-precise measurement of $\sin^2 \theta_w$
  - **MREX:** Ultra-precise measurement of $R_n - R_p$ for ^{208}Pb
- MREX will improve on the precision of the asymmetry measured in PREX-II
- Both experiments to run after the completion of MESA

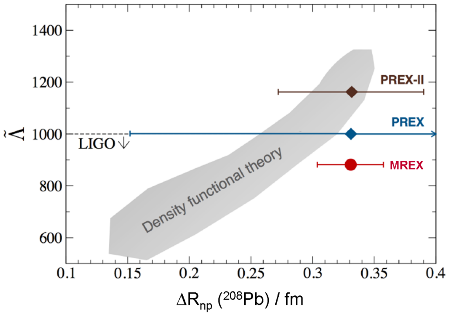

Above: Projected precision for PREX-II and MREX experiments compared to the range of neutron radii predicted by DFT models. Reproduced from Becker et al., Eur. Phys. J. A, ***54*** *(2018), 11*

Compton Backup

Compton Polarimetry

Images Credit: *D. Gaskell (2019)*

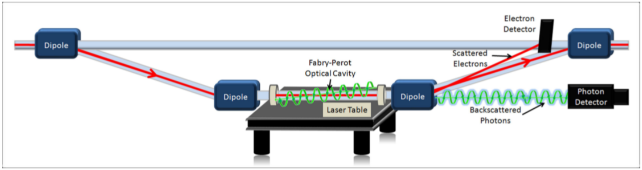

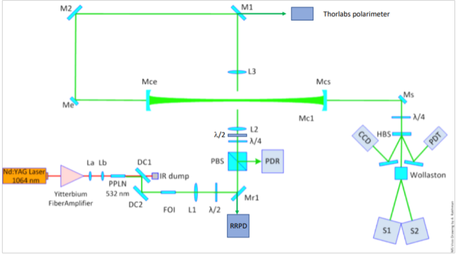

Optics table device layout

- Polarimeter consists of:
  - Magnetic chicane to steer beam
  - Fabry-Perot cavity on laser table
  - Photon calorimeter
  - High-speed DAQ system
- Laser/Amp outputs at λ=1064 nm, but is doubled to λ=532 nm
- Laser polarization measured on table

Polarimeter Laser

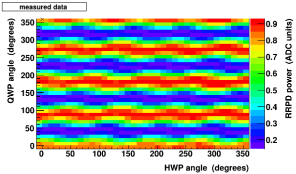

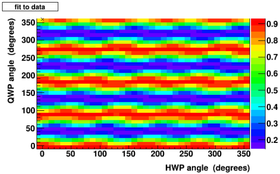

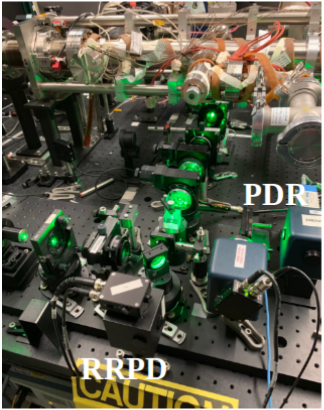

- Laser polarization achieved with combination of half waveplates and quarter waveplates
- Retro-reflected photodiode (RRPD) power anti-correlated with degree of circular polarization (DOCP)
- Laser polarization highly controlled and measurable
- Laser input state can become arbitrary

Laser Cycling

- To handle shifts in background, we periodically flip off the laser
- Backgrounds calculated on cycle-to-cycle basis
- 1 cycle = a laser-on period, sandwiched by two laser off periods

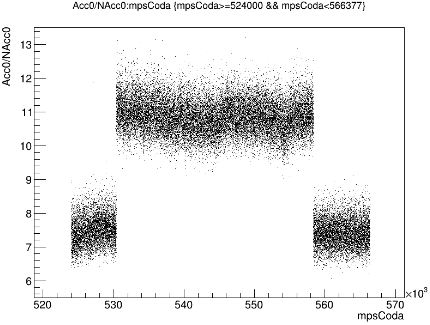

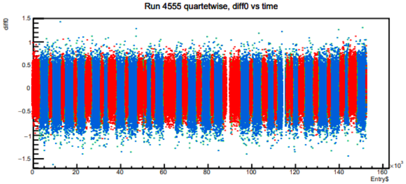

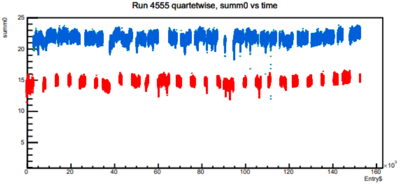

Top: Plot of helicity correlated differences vs time for one PREX-II run
Bottom: Plot of sums for same time period

In each plot, low variation of the integrated signal is likely indicative of healthy data.

In all plots, blue represents laser-on periods, red represents laser-off.

Data shown here was taken over a ≈90 minute period.

Laser Polarization Model

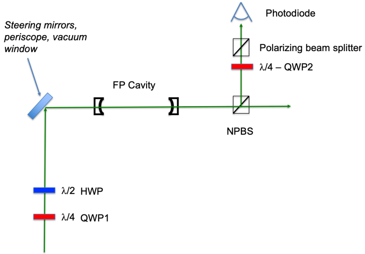

Before run:

- NPBS used to used to characterize DOCP in-cavity
- Complicated by birefringence of cavity mirrors
- Entrance scans, exit scans, cavity scans. . .

During run:

- Additional verification: running off 100%
- QWP/HWP changed for multiple snails to alter DOCP
- Saw polarization magnitude decrease
- Laser systematic still being calculated!
  - Study on birefringence parameters still pending

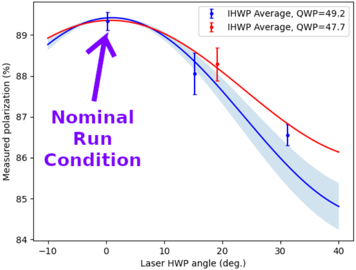

Compton Photon Detector

Images Credit: *J. C. Cornejo (2019)*

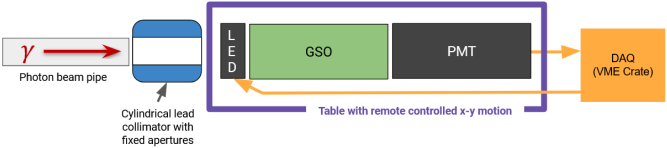

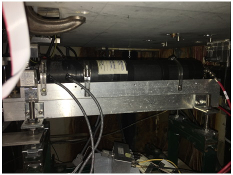

- Detector Components:
    - Pb Collimator
    - Pb Sync Shield
    - GSO scintillator
    - PMT and DAQ readout
- Signals read out per rapidly-flipping helicity state
- Measure helicity-correlated asymmetry
- LED's allow for *in-situ* detector tests

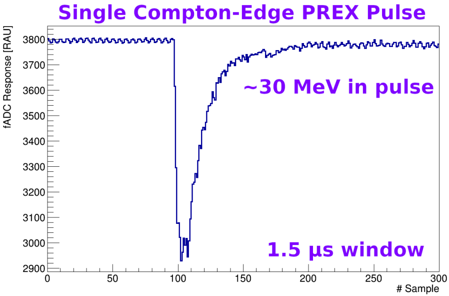

Example photon pulse with energy matching the PREX Compton-edge. The CREX Compton edge photons had about 4x greater energy

Polarimetry Measurement: Integrating Method

How to measure a Compton Asymmetry: Integrate the signal over pedestal per helicity state.
Measure signal S, for each laser state ON, OFF and helicity state $+, -$.
Helicity pattern difference (Δ), sum (Y), and asymmetry $(\mathcal{A})$ distributions are calculated:

$$\Delta_{ON} = S^{+}_{ON} - S^{-}_{ON}$$

$$\Delta_{OFF} = S^{+}_{OFF} - S^{-}_{OFF}$$

$$Y_{ON} = S^{+}_{ON} + S^{-}_{ON}$$

$$Y_{OFF} = S^{+}_{OFF} + S^{-}_{OFF}$$

$$\mathcal{A}_{ON} = \frac{\Delta_{ON}}{Y_{ON} - \langle Y_{OFF} \rangle}$$

$$\mathcal{A}_{OFF} = \frac{\Delta_{OFF}}{\langle Y_{ON} \rangle - \langle Y_{OFF} \rangle}$$

$$\mathcal{A}_{exp} = \langle \mathcal{A}_{ON} \rangle - \langle A_{OFF} \rangle = \mathcal{P}_e \mathcal{P}_\gamma \langle \mathcal{A}_l \rangle$$

With laser DOCP $\mathcal{P}_\gamma$, energy-weighted average analyzing power $\langle \mathcal{A}_l \rangle$, and beam polarization $\mathcal{P}_e$.

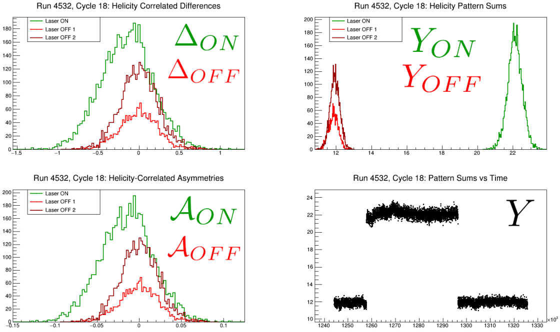

Compton Spectra

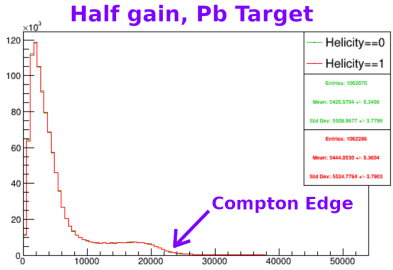

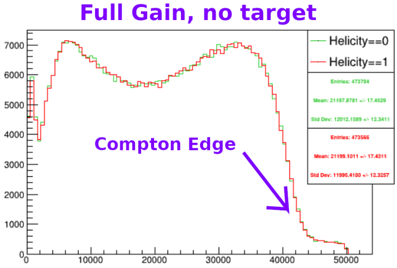

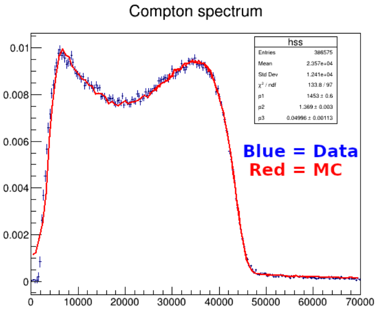

- Spectrum of integrated pulse energy
- MC fit to data well
    - Also can extract photon beam position systematic from fits
- Pb target: high backgrounds due to neutrons and detector Gd content
- Ca target: much lower backgrounds

Detector Corrections

Nonlinearity

- 1 kHz pulser system w/ load = PREX signal
  - Track $Yield(var + \Delta) - Yield(var)$
- Nonlinearity out to 2*CE
- Very small analyzing power correction (≈0.08% for PREX)

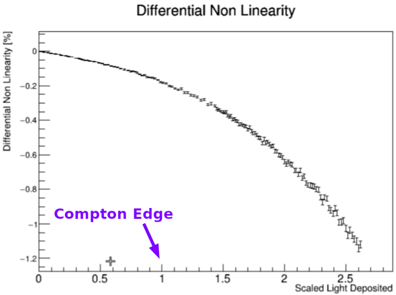

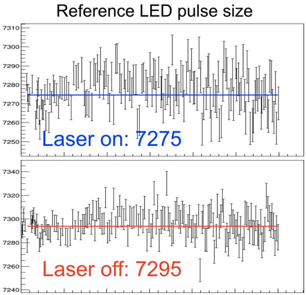

Gain Shift

- Evidence of small change in pulse size with background signal size
- Nonzero shift necessitates dynamic correction
- Bench tests of gain shift done
  - Analysis yielded correction factor for $\mathcal{A}_{exp}$

Left: *Evidence of a gain shift from a linearity run taken during beam operations*